Eur. Phys. J. B **58**, 475–481 (2007)
DOI: 10.1140/epjb/e2007-00240-2

THE EUROPEAN PHYSICAL JOURNAL B

The underdamped Josephson junction subjected to colored noises

L.R. Nie[1,2] and D.C. Mei[1,a]

[1] Department of Physics, Yunnan University, Kunming 650091, P.R. China
[2] Science School, Kunming University of Science and Technology, Kunming 650051, P.R. China

Received 15 November 2006 / Received in final form 8 August 2007
Published online 14 September 2007 –

Abstract. The properties of the underdamped Josephson junction subjected to colored noises were investigated with large and small phase difference (ϕ). For the case of the large ϕ, we found numerically that: (i) the probability distribution function of ϕ exhibits monostability $\rightarrow$ bistability $\rightarrow$ monostability transitions as the autocorrelation rate (λ) of a colored noise increases; (ii) in the bistability region the multiplicative noise drives the phase difference to turn over periodically; (iii) the slope K of the linear response of the junction potential difference ($\langle V \rangle$) can be somewhat reduced by means of tuning an optimal λ; (iv) the amplitude of ϕ in response to external sinusoidal signals changes with λ. For the case of small ϕ, after deriving the analytical expressions of the potential difference amplitude ($\langle V \rangle_{max}$) and the K in the presence of a dichotomous noise, we found nonmonotonic behavior of $\langle V \rangle_{max}$ and the slope K as a function of λ.

PACS. 05.40.-a Fluctuation phenomena, random processes, noise, and Brownian motion – 85.25.Cp Josephson devices – 87.15.Aa Theory and modeling; computer simulation

1 Introduction

Much recent research work [1–3] has been devoted to the study of Brownian particles in periodic potentials. Of course, the study of Josephson superconducting junctions becomes increasingly important not only because experimentally it can be fabricated into a variety of superconducting devices [4,5], but also because theoretically one can explain some phenomena by means of the methods of statistical physics, e.g., net voltage phenomenon [6,7], E–j relationship [8], noise-enhanced diffusion [9], V–I characteristics [1,10] and so on. Yet these discussions have been confined to overdamped circumstances. However, two noise-induced effects, namely resonant activation and noise-enhanced stability, were experimentally observed in underdamped Josephson junctions [11,12] and theoretically predicted in an overdamped Josephson junction [13].

In the underdamped case, one always subjects the Brownian particles of periodic potentials to Gaussian white noise due to temperature [14,15]. Brownian motion of an array of harmonically coupled particles subject to a periodic substrate potential and Gaussian white noise was studied in reference [16]. Critical hysteresis in a tilted washboard potential driven by Gaussian white noise was performed by Borromeo et al. [17]. We note that different noise sources, such as additive or multiplicative noises, white or colored noises, are worth considering. References [18,6,19] take a dichotomous noise into account to study the Josephson junction for a large range of phase differences, and obtain many significant results. However they also restrict the discussed models to overdamped cases. Much less effort has been made in studying the influence of colored noises on the underdamped Josephson junction.

Stochastic resonance (SR), a phenomenon resulting from the combination of nonlinear dynamic systems with a random force and an external periodic signal [20], has received much attention due to its application in biology, physics, and chemistry [21]. The analysis of SR in linear systems was previously restricted to an overdamped oscillation with multiplicative colored noises [22]. For an underdamped oscillation, reference [23] examined a bistable potential with the Gaussian additive white noises in view of moments, not with colored or dichotomous noises. For an underdamped Brownian particle moving in a periodic potential, there is no conventional SR. Due to the unbound motion in the periodic potential, transition probability decays algebraically and there is no persistent synchronized hopping. However the noise-induced enhancement of the diffusion constant exhibits a SR-like behavior [24].

This paper aims to address the effects of colored noises on the underdamped Josephson junction. In Section 2 the

[a] e-mail: meidch@ynu.edu.cn

properties of the Josephson junction in the case of large phase difference ϕ, e.g., the stationary probability distribution function (PDF) of ϕ, the $\langle V\rangle - I$ characteristics and the harmonic oscillations under different autocorrelation rates of colored noises, are obtained. In Section 3 the analytical characteristics of the Josephson junction subject to dichotomous noises in the case of small phase difference are presented. In Section 4 we give the conclusions.

2 The large phase difference case

The Josephson tunneling junction consists of two superconductors which are separated by a thin oxide layer [15]. If it is driven by a fixed current and an external periodic signal, according to references [25,26], the form of the pendulum equation with a sine term can be obtained:

$$\frac{\hbar}{2e}C\ddot{\phi} + \frac{\hbar}{2eR}\dot{\phi} + J_0 \sin\phi = I + \eta(t) + a\sin\Omega t,$$
$$\dot{\eta} = -\lambda\eta + \lambda\Gamma(t), \qquad (1)$$

where $\eta(t)$ and $\Gamma(t)$ are Gaussian noises with zero mean, and

$$\langle\eta(t)\eta(t')\rangle = E^2\exp(-\lambda \mid t - t' \mid),$$
$$\langle\Gamma(t)\Gamma(t')\rangle = 2D\delta(t-t'), \qquad (2)$$

where R, J_0 and I are the junction resistance, the maximum Josephson current and the total current; ϕ and C represent the phase difference and the capacitance between the two superconductors respectively. Overdots in equation (1) denote derivatives with respect to time. $\eta(t)$ is modeled here by the well-known Ornstein-Uhlenbeck process with an exponential correlation function. λ denotes its autocorrelation rate. The intensity of the colored noise $\eta(t)$ is equal to D/λ (i.e., $E^2 = D/\lambda$), and E is a constant. D is the intensity of Gaussian white noise $\Gamma(t)$.

If environmental perturbations exist, such as perturbation of the electromagnetic fields, external vibrations, and so on, they will give rise to a fluctuation of the critical current in the Josephson junction [6]. Fluctuations of external parameters are expressed by a multiplicative noise [1]. As in reference [6], we describe this fluctuation by a stochastic external parameter$J_0+\sigma\eta(t)$, in which $\eta(t)$ is the stochastic force with the same statistical properties as in equations (2) and σ is a constant. Thus equation (1) can be rewritten in the form:

$$\frac{\hbar}{2e}C\ddot{\phi} + \frac{\hbar}{2eR}\dot{\phi} + J_0\sin\phi + (\sigma\sin\phi - 1)\eta(t) = I + a\sin\Omega t. \qquad (3)$$

The Fokker-Planck-equation corresponding to equation (3) is rather difficult to solve analytically even for the stationary case without a periodic signal. But the time evolution of the phase difference and the potential difference in equation (3) can be simulated by means of Euler arithmetic. The time step is chosen to be small enough to realize simulation processes as the very tiny inertial mass of the Josephson junction results in very rapid time evolution. The Box-Mueller algorithm is used to generate Gaussian noise from two random numbers which are uniformly distributed over the unit interval.

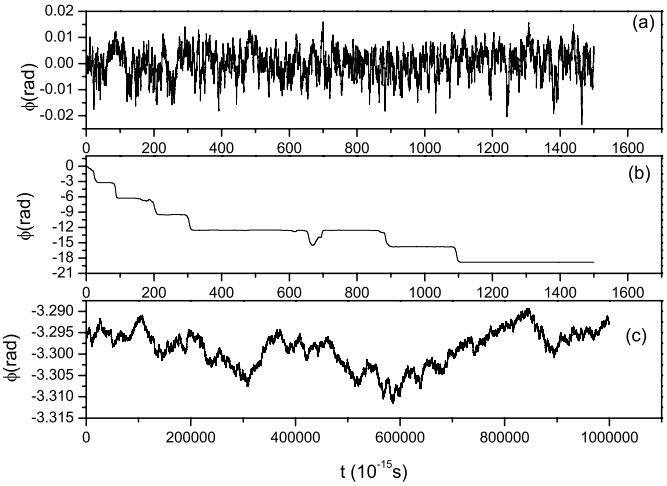

Fig. 1. The time evolution of phase differences at different correlation rates λ: 10^{17}, 10^{13} and 10^6 for (a)–(c) respectively, with $E = 1$, $J_0 = 10$ A, $\sigma = 20$, $C = 0.01$ pF, $R = 0.01$ Ω, $I = 0$ and $a = 0$. The time step is 10^{-18} s for (a) and (b), 10^{-16} s for (c).

2.1 The stationary probability distribution function

The time evolution of ϕ have been stochastically simulated by means of equation (3), and the results are shown in Figure 1. Figure 1 indicates that the colored noise affects the variation of the phase difference to a large degree. In the constant product of $D\lambda$, the Brownian particles are either in a "locking state" or a "running state" as λ changes. In the "locking state" the particles are bound in a very small range of ϕ, whereas in the "running state" they cover distances of several periods in the clockwise direction. In order to clearly show the characteristics of ϕ in the "running state", we simulated the angle displacement and its PDF during 10^{-10} s via equation (3). Simulation results are plotted in Figure 2. Figure 2a reflects the variation scales of ϕ. In terms of whether the particles are in the locking state or in the running state, the correlation rates are divided into three regions. In the process of simulation, we further found that: in the second region the PDF of ϕ displays bistablity (see Fig. 2b). If ϕ is drawn back to the range of -2π to 0, one stable state appears near about $\phi = 0$, and the other one near $-\pi$; in the first region the particles are randomly either at stable state 1 ($\phi = 0$) or stable state 2 ($\phi = -\pi$); but in the third region the particles are only at stable state 1. In other words the particles experience the transitions of monostability $\rightarrow$ bistability $\rightarrow$ monostability as the autocorrelation rate (λ) of the colored noise increases.

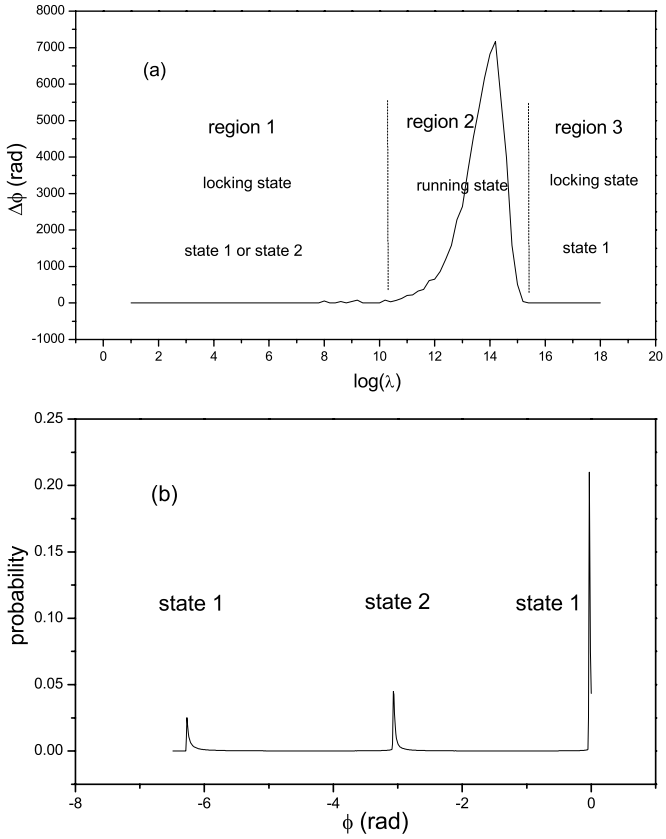

Fig. 2. (a) The angle displacement during 10^{-10} s versus λ. The other parameters are: $E = 1$, $J_0 = 10$ A, $\sigma = 20$, $C = 0.01$ pF, $R = 0.01\ \Omega$, $I = 0$, $a = 0$ and 10^{-18} s time step. (b) The stationary PDF of ϕ at $\lambda = 10^{13}$; the other parameters are: $E = 1$, $J_0 = 10$ A, $\sigma = 20$, $C = 0.01$ pF, $R = 0.01\ \Omega$, $I = 0$, $a = 0$ and 10^{-18} s time step.

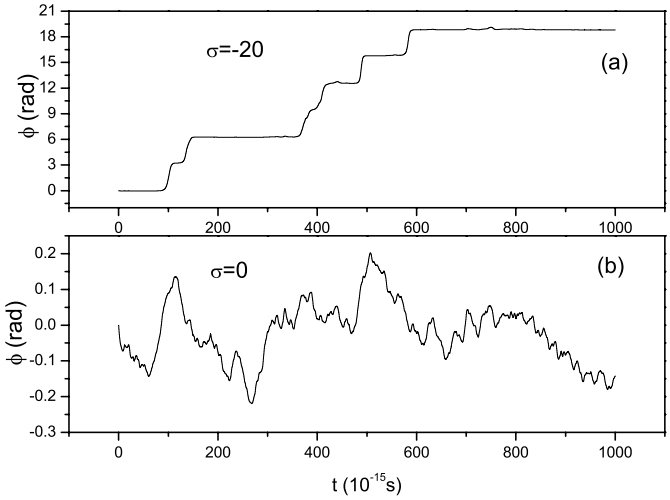

Fig. 3. The effect of multiplicative colored noises on the time evolution of phase differences at $\lambda = 10^{13}$. The other parameters are the same as in Figure 1.

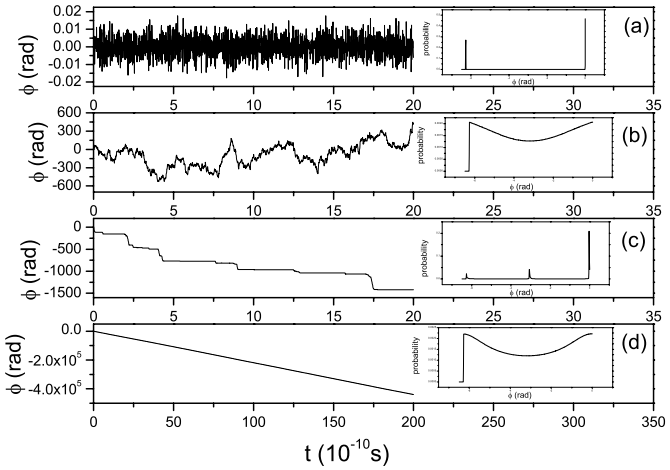

Fig. 4. The time evolution of phase differences at different correlation rates λ: 10^{17}, 10^{13}, 10^{10} and 10^{5} for (a)–(d) respectively, with $C = 100$ pF. The other parameters are the same as in Figure 1. These inner panels are their corresponding stationary PDF of ϕ.

What is the reason why the phase difference in the second region turns over periodically? We altered the coefficient σ of multiplicative noises to simulate the time evolution of ϕ at the "running state" as done in Figure 2, and the results are shown in Figure 3. From Figure 3 we found that the turnover of ϕ doesn't take place as $\sigma = 0$, and that ϕ turns over counterclockwise as $\sigma = -20$. Furthermore, the larger the value of σ, the faster ϕ turns over. It means that environmental perturbations (or multiplicative noises) control the rotation direction of ϕ without external torques. The analogous phenomenon appeared in reference [27].

As the junction capacitance increases, i.e., $C = 100$ pF, the bistability regime still appears if λ takes the value of 10^{10} (see Fig. 4c). Yet in the case of smaller λ, ϕ undergoes uniform and continuous turnover and the locking state is lost due to the larger inertial mass (see Fig. 4d).

In equation (3), a single random variable is introduced to reflect both environmental and thermal perturbations, which corresponds to the strongly correlated case between multiplicative and additive noises. In order to study the influence of the correlation on the bistability regime, we consider two sources of colored noises

$$\begin{aligned}
&\frac{\hbar}{2e}C\ddot{\phi}+\frac{\hbar}{2eR}\dot{\phi}+J_0\sin\phi+\sigma\sin\phi\eta_1(t)-\eta_2(t)=I+a\sin\Omega t,\\
&\dot{\eta_1}=-\lambda\eta_1+\lambda\Gamma_1(t),\\
&\dot{\eta_2}=-\lambda\eta_2+\lambda\Gamma_2(t),\\
&\langle\eta_i(t)\eta_i(t')\rangle=E^2\exp(-\lambda\mid t-t'\mid),\quad i=1,2\\
&\langle\eta_i(t)\eta_j(t')\rangle=sE^2\exp(-\lambda\mid t-t'\mid),\quad i,j=1,2,\quad i\neq j\\
&\langle\Gamma_i(t)\Gamma_j(t')\rangle=2D\delta_{ij}\delta(t-t'),\quad i,j=1,2
\end{aligned}\tag{4}$$

where s is the correlated strength between the two sources of colored noise. Simulating stochastically equation (4), we found that the bistability regime at any correlated strength still exists and s only changes the turnover direction and speed of ϕ (see Fig. 5).

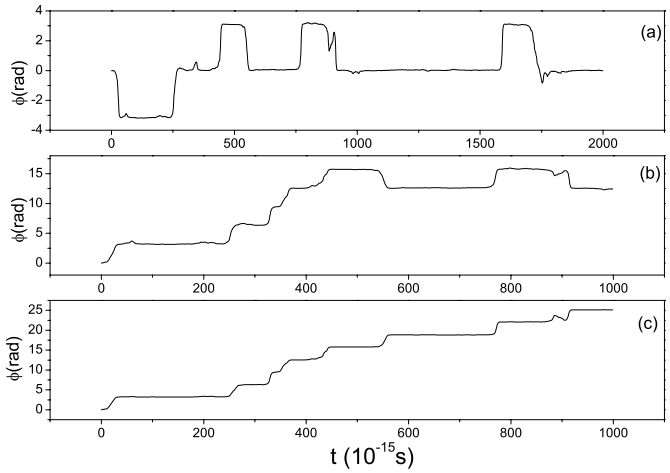

Fig. 5. The time evolution of phase differences at different correlated strengths s: 0.7, 0 and -1 for (a)–(c). The other parameter values are the same as in Figure 1b.

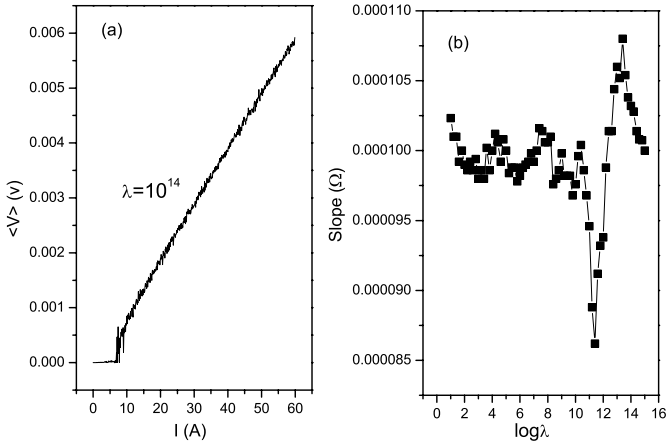

Fig. 6. (a) and (b) are the curve of $\langle V\rangle - I$ at $\lambda = 10^{14}$ and the relationship between the slope of the beeline $\langle V\rangle - I$ and λ respectively, $E = 1$, $J_0 = 10$ A, $\sigma = 20$, $C = 0.1$ μF, $R = 0.01$ Ω, $a = 0$ and 10^{-18} s time step.

2.2 $\langle$V$\rangle$ − I characteristics

In the study of the Josephson junction, a paramount physical quantity is the average potential difference across the oxide layer of the Josephson junction, defined as:

$$\langle V\rangle = \frac{\hbar}{2e}\langle\dot{\phi}\rangle. \tag{5}$$

When the external torque (or the total current) I is small, the pendulum can perform only small oscillations around its equilibrium point, while for sufficiently large I, the pendulum is able to execute complete rotations. This point is to some extent visible in Figure 6a which comes from the simulation of equation (3). From Figure 6a, we can see that the threshold of I is less than J_0, which differs from that in overdamped cases. Above the threshold, the phase difference ϕ can counterclockwise turn over continuously and uniformly in a linear region, so the potential difference varies linearly with the total current. Below the threshold, $\langle V\rangle$ is independent of I, which is consistent with the following analytical result in the small phase difference case. In order to study the effect of noise on the $\langle V\rangle - I$ characteristics, the slope K of the $\langle V\rangle - I$ beeline as a function of λ is also simulated. The results plotted in Figure 6b show that the slope K can only be slightly reduced by properly tuning the autocorrelation rate λ.

2.3 Harmonic oscillation

Let us next consider the case in which a small sinusoidal periodic signal is input into the underdamped Josephson without the external torque I. The simulated results of the three regions in Figure 2b are shown in Figure 7. In the two monostability regions the phase differences sine-oscillates distinctly periodically with time in equal frequencies and different amplitudes while the signal becomes blurred a little in the bistablity region. It is very obvious that the

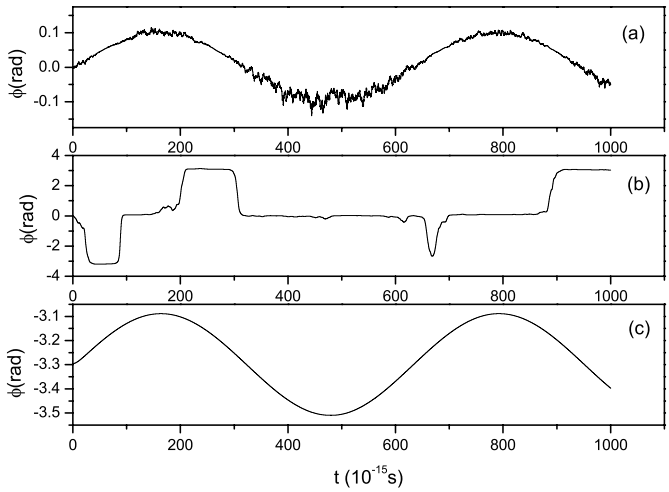

Fig. 7. The time evolution of phase differences at different correlation rates λ: 10^{17}, 10^{13} and 10^{6} for (a)–(c) respectively, with $E = 1$, $J_0 = 10$ A, $\sigma = 20$, $C = 0.01$ pF, $R = 0.01$ Ω, $I = 0$, $a = 1$, $\Omega = 10^{13}$ s^{-1} and 10^{-18} s time step.

particles in the "running state" no longer rotate continuously in a clockwise direction, but converge periodically to a quasi-square wave with the largest amplitude. Thus different autocorrelation rates produce different periodic amplitudes. Although conventional SR does not occur in this case due to the unbound motion in the periodic potential, the phase difference amplitude is very likely to present an SR-like behavior. This phenomena will become more pronounced in the following small phase difference case.

3 The small phase difference case

The most significant property of the Josephson junction is the threshold behavior of the potential difference $\langle V\rangle$. Here we mainly discuss the properties of $\langle V\rangle$ during the

small phase difference range. Through the above analysis, we knew that in the stationary state whether the phase difference ϕ is positioned either in the stable state 1 or in the stable state 2 makes a small sway. When the total junction current I and the sinusoidal signal in equation (1) are very small, the small angle approximation $\sin\phi \simeq \phi$ can be used. Thus equation (1) can be rewritten as:

$$\frac{\hbar}{2e}C\ddot{\phi} + \frac{\hbar}{2eR}\dot{\phi} + J_0\phi + (\sigma\phi - 1)\eta(t) = I + a\sin\Omega t. \quad (6)$$

In order to obtain the analytical solution to equation (6), $\eta(t)$ is assumed to be a dichotomous noise, a random stationary Markovian process consisting of jumps between two values $\eta(t) = -E, E$ with equal stationary probability 1/2. There are both multiplicative and additive noises in equation (6). Adopting the method of reference [28], first averaging both sides of equation (6) and then using twice the Shapino-Loginov differential formula [29], we easily get a fourth-order differential equation for variable ϕ:

$$\begin{aligned}
&\frac{d^4\langle\phi\rangle}{dt^4} + 2\left(\lambda + \frac{1}{RC}\right)\frac{d^3\langle\phi\rangle}{dt^3} + \left(\lambda^2 + \frac{3}{RC}\lambda\right. \\
&\quad \left. + \frac{4eJ_0}{\hbar C} + \frac{1}{R^2C^2}\right)\frac{d^2\langle\phi\rangle}{dt^2} \\
&\quad + \frac{1}{RC}\left[\lambda^2 + \left(\frac{1}{RC} + \frac{4eRJ_0}{\hbar}\right)\lambda\right. \\
&\quad \left. + \frac{4eJ_0}{\hbar C}\right]\frac{d\langle\phi\rangle}{dt} + \left[\frac{2eJ_0}{\hbar C}\left(\lambda^2 + \frac{1}{RC}\lambda\right)\right. \\
&\quad \left. + \left(\frac{2e}{\hbar C}\right)^2\left(J_0^2 - \sigma^2E^2\right)\right]\langle\phi\rangle = \\
&\frac{2ea}{\hbar C}\left(\lambda^2 + \frac{1}{RC}\lambda + \frac{2eJ_0}{\hbar C} - \Omega^2\right)\sin\Omega t \\
&\quad + \left(2\lambda + \frac{1}{RC}\right)\frac{2ea\Omega}{\hbar C}\cos\Omega t \\
&\quad + \frac{2eI}{\hbar C}\left(\lambda^2 + \frac{1}{RC}\lambda + \frac{2eJ_0}{\hbar C}\right) - \left(\frac{2eE}{\hbar C}\right)^2\sigma. \quad (7)
\end{aligned}$$

Here our aim is to look for the response of the system to external environments. Therefore it is necessary to find the special solution to equation (7) corresponding to the sinusoidal signal and the external torque I.

Let

$$\frac{2eJ_0}{\hbar C}\left(\lambda^2 + \frac{1}{RC}\lambda\right) + \left(\frac{2e}{\hbar C}\right)^2(J_0^2 - \sigma^2E^2) = C_1 \neq 0, \quad (8)$$

the solution of equation (7) can be approximated by

$$\langle\phi\rangle_{ex} = A\sin(\Omega t + \varphi) + B. \quad (9)$$

After inserting equation (9) into equation (7), the three coefficients of equation (9) can be obtained:

$$\begin{aligned}
A &= \left(\frac{C_4^3 + C_5^2}{C_2^2 + C_3^2}\right)^{1/2}, \\
\tan\varphi &= \frac{C_2C_5 - C_3C_4}{C_3C_5 + C_2C_4}, \\
B &= \frac{C_6}{C_1}, \quad (10)
\end{aligned}$$

where

$$\begin{aligned}
C_2 &= \Omega^4 - \left(\lambda^2 + \frac{3}{RC}\lambda + \frac{4eJ_0}{\hbar C} + \frac{1}{R^2C^2}\right)\Omega^2 + C_5, \\
C_3 &= -2\left(\lambda + \frac{1}{RC}\right)\Omega^3 \\
&\quad + \frac{1}{RC}\left[\lambda^2 + \left(\frac{1}{RC} + \frac{4eRJ_0}{\hbar}\right)\lambda + \frac{4eJ_0}{\hbar C}\right]\Omega, \\
C_4 &= \frac{2ea}{\hbar C}\left(\lambda^2 + \frac{1}{RC}\lambda + \frac{2eJ_0}{\hbar C} - \Omega^2\right), \\
C_5 &= \left(2\lambda + \frac{1}{RC}\right)\frac{2ea\Omega}{\hbar C}, \\
C_6 &= \frac{2eI}{\hbar C}\left(\lambda^2 + \frac{1}{RC}\lambda + \frac{2eJ_0}{\hbar C}\right) - \left(\frac{2eE}{\hbar C}\right)^2\sigma. \quad (11)
\end{aligned}$$

So the potential difference across the oxide layer of a Josephson junction can be expressed as

$$\begin{aligned}
\langle V\rangle &= \frac{\hbar}{2e}\langle\dot{\phi}\rangle_{ex} = \frac{\hbar\Omega A}{2e}\cos(\Omega t + \varphi) \\
&= \langle V\rangle_{max}\cos(\Omega t + \varphi). \quad (12)
\end{aligned}$$

The above equation indicates that the potential difference also displays a periodic oscillation with the external signal in equal frequency and is independent of the current I. The slope of the small segment near the origin in Figure 6a verifies this independence.

The amplitude a of the sinusoidal signal is equal to 0.1 A small enough to guarantee the approximation $\sin\phi \simeq \phi$. Using equations (10), (11) and (12), we generated curves of the relationship of $\langle V\rangle_{max}$ with the autocorrelation λ under various inertial masses and electrical resistances, which are displayed in Figure 8, where $\langle V\rangle_{max}$ exhibits nonmonotonic behaviour. The optimal λ being chosen, a maximum amplitude of $\langle V\rangle$ can be obtained. The optimal λ value increases with decreasing junction capacitance. Yet the abscissa λ corresponding to the peak in Figure 6b does not vary markedly with the junction resistance R, Furthermore, the peak value of $\langle V\rangle$ amplitude almost approaches saturation after R is greater than about 0.05 Ω.

In the other case:

$$C_1 = 0 \quad \text{and} \quad a = 0, \quad (13)$$

the special solution of equation (7) is assumed to be

$$\langle\phi\rangle_{ex} = Qt, \quad (14)$$

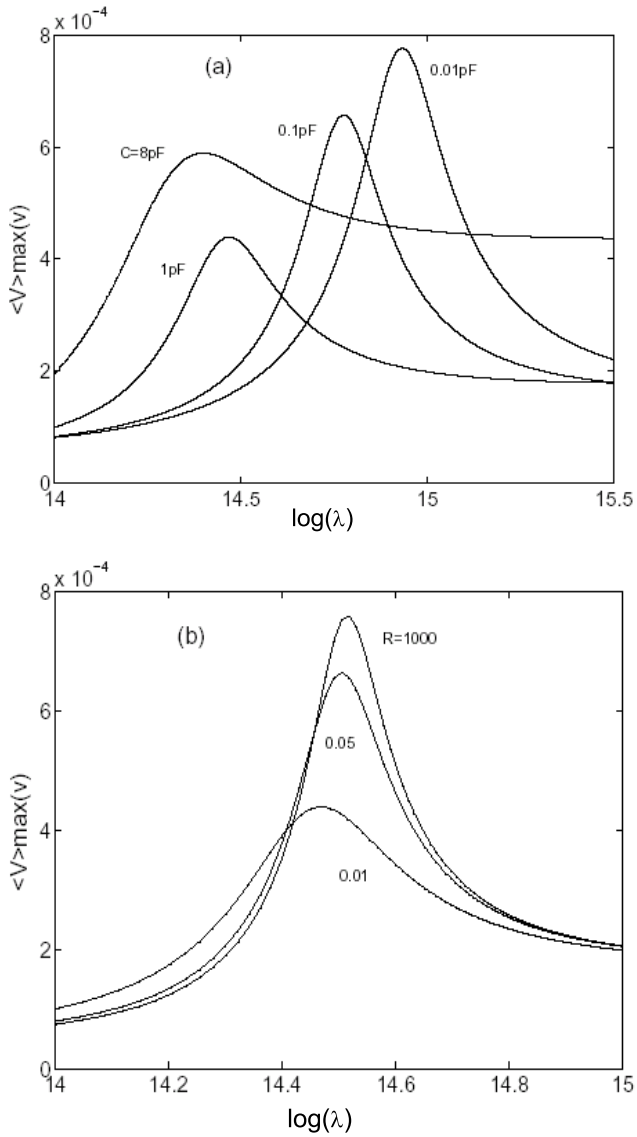

Fig. 8. The amplitude of the potential difference as a function of the logarithm of λ, $J_0 = 10$ A, $\sigma = 20$, $a = 0.1$ A, $\Omega = 10^{13}$ s^{-1} and $E = 1$. (a) Corresponds to the amplitude of the potential difference for different capacitance values, with $R = 0.01$ Ω; (b) corresponds to that for different resistance values, with $C = 1$ pF.

with

$$Q = \frac{C_6}{C_1'}, \qquad C_1' = \frac{1}{RC}\left[\lambda^2 + \left(\frac{1}{RC} + \frac{4eRJ_0}{\hbar}\right)\lambda + \frac{4eJ_0}{\hbar C}\right]. \tag{15}$$

The potential difference takes the form:

$$\langle V\rangle = \frac{\hbar Q}{2e} = KI + \langle V\rangle_0, \tag{16}$$

where K and $\langle V\rangle_0$ are respectively the slope and intercept of the beeline $\langle V\rangle - I$. The analytical expression of K reads:

$$K = \frac{\lambda^2 + \frac{1}{RC}\lambda + \frac{2eJ_0}{\hbar C}}{\lambda^2 + (\frac{1}{RC} + \frac{4eRJ_0}{\hbar})\lambda + \frac{4eJ_0}{\hbar C}}R. \tag{17}$$

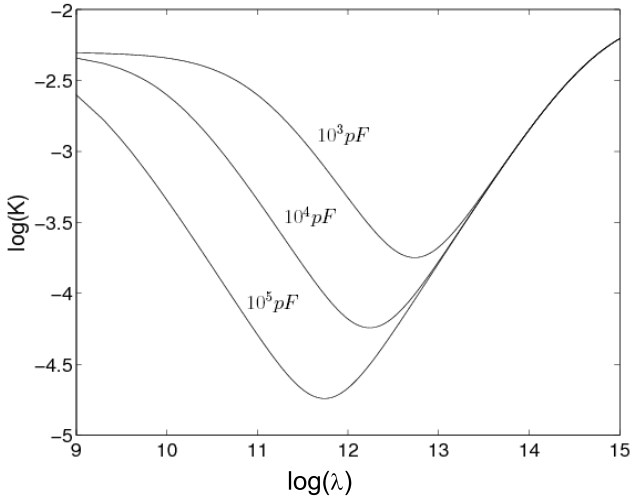

Fig. 9. The logarithm of the slope K of the beeline as a function of the logarithm of λ at different capacitance values for $J_0 = 10$ A, $R = 0.01$ Ω.

By means of equation (17), the nonmonotonic behavior of K as a function of λ, under different inertial masses, is shown in Figure 9. Choosing an optimal λ, we can obtain a minimum value of K. The larger the junction capacitance, the smaller the minimum value. The analogous relation between K and λ occurs equally in the large phase difference case (see Fig. 6b).

4 Conclusions

The effect of multiplicative colored noise on the underdamped Josephson junction has been investigated. For the large phase difference case, stochastic simulations were performed, while for the small phase difference case, analytical solutions to multiplicative dichotomous noises were derived. It is the very small inertial mass of the junction that results in high speed time-evolution, small effective noise intensity or extreme large effective autocorrelation.

For the case of large phase difference ϕ, without external torques and signals, the ϕ undergoes the transitions of monostability → bistability → monostability as the autocorrelation rate (λ) of the colored noise increases. The rotational direction of ϕ in the "running state" of the bistability region is contrilled by the coefficient of multiplicative colored noise. The larger inertial mass may lead to the smaller threshold. Below the threshold of the junction total current I, the junction potential difference $\langle V\rangle$ does not affect I. The slope of $\langle V\rangle - I$ above the threshold is reduced to some extent at an optimal autocorrelation rate (λ). For the case of small phase difference ϕ, the amplitude of $\langle V\rangle$ in response to a small sinusoidal signal exhibits a resonance-like behavior. When $C_1 \neq 0$, $\langle V\rangle$ is independent of I. When $C_1 = 0$, the minimum slope of $\langle V\rangle - I$ results from a moderate λ, and is influenced by the Brownian inertial mass.

This work was supported by the Natural Science Foundation of Yunnan province of China (2006A0002M).

References

1. M. Gitterman, V. Berdichevsky, Phys. Rev. E **65**, 011104 (2001)
2. A.A. Dubkov, B. Spagnolo, Phys. Rev. E **72**, 041104 (2005)
3. J. Luczka, T. Czernik, P. Hänggi, Phys. Rev. E **56**, 3968 (1997)
4. Y. Makhlin, G. Schön, A. Shnirman, Rev. Mod. Phys. **73**, 357 (2001)
5. H. Xu, A.J. Berkley, R.C. Ramos, M.A. Gubrud, P.R. Johnson, F.W. Strauch, A.J. Dragt, J.R. Anderson, C.J. Lobb, F.C. Wellstood, Phys. Rev. B **71**, 064512 (2005)
6. Jing-Hui Li, Zu-Qia Huang, Phys. Rev. E **58**, 139 (1998)
7. Jing-Hui Li, Phys. Rev. E **67**, 061110 (2003)
8. Y. Jia, S.N. Yu, J.R. Li, Phys. Rev. E **63**, 052101 (2001); Baoxing Chen, Jinming Dong, Phys. Rev. B **44**, 10206 (1991)
9. P. Reimann, C. Van den Broeck, H. Linke, P. Hänggi, J.M. Rubi, A. Pérez-Madrid, Phys. Rev. Lett **87**, 010602 (2001)
10. A. Barone, G. Paterno, *Physics and Applications of the Josephson Effect* (Wiley, New York, 1982)
11. Y. Yu, S. Han, Phys. Rev. Lett. **91**, 127003 (2003)
12. G. Sun et al., *Thermal Escape from a Metastable State in Periodically Driven Josephson Junction*, e-print `arXiv:cond-mat/0602401` (2006)
13. A.L. Pankratov, B. Spagnolo, Phys. Rev. Lett. **93**, 177001 (2004)
14. D. Koelle, R. Kleiner, F. Ludwig, E. Dantsker, J. Clarke, Rev. Mod. Phys. **71**, 631 (1999)
15. H. Risken, *The Fokker-Planck Equation* (Springer-Verlag, Berlin, 1984)
16. Zhigang Zheng, Bambi Hu, Gang Hu, Phys. Rev. E **58**, 7085 (1998)
17. M. Borromeo, G. Costantini, F. Marchesoni, Phys. Rev. Lett. **82**, 2820 (1999)
18. V. Berdichevsky, M. Gitterman, Phys. Rev. E **56**, 6340 (1997)
19. S.H. Park, S. Kim, C.S. Ryu, Phys. Lett. A **225**, 245 (1997)
20. R. Benzi, S. Sutera, A. Vulpiani, J. Phys. A **14**, L453 (1981); C. Nicolis, Tellus **34**, 1 (1982)
21. L. Gammaitoni, P. Hänggi, P. Jung, F. Marchesoni, Rev. Mod. Phys. **70**, 223 (1998)
22. V. Berdichevsky, M. Gitterman, Europhys. Lett. **36**, 161 (1996); A.V. Barzykin, K. Seki, F. Shibata, Phys. Rev. E **57**, 6555 (1998)
23. Y.M. Kang, J.X. Xu, Y. Xie, Phys. Rev. E **68**, 036123 (2003)
24. Y.W. Kim, W. Sung, Phys. Rev. E **57**, 6237 (1998)
25. Y.M. Ivanchenko, L.A. Zil'berman, Sov. Phys. JETP **28**, 1272 (1969)
26. V. Ambegaokar, B.I. Halperin, Phys. Rev. Lett. **22**, 1364 (1969)
27. B. Lindner, L. Schimansky-Geier, P. Reimann, P. Hänggi, M. Nagaoka, Phys. Rev. E **59**, 1417 (1999)
28. M. Gitterman, Phys. Rev. E **67**, 057103 (2003)
29. V.E. Shapino, W.M. Loginov, Physica A **91**, 563 (1978)